Comput. Methods Appl. Mech. Engrg. 233–236 (2012) 152–163

Contents lists available at SciVerse ScienceDirect

Comput. Methods Appl. Mech. Engrg.

journal homepage: www.elsevier.com/locate/cma

# Fast multipole boundary element method for the Laplace equation in a locally perturbed half-plane with a Robin boundary condition

Carlos Pérez-Arancibia [a,*], Pedro Ramaciotti [b], Ricardo Hein [a], Mario Durán [b]

[a] Ingenieros Matemáticos Consultores Asociados S.A. (INGMAT), Santiago, Chile
[b] Centro de Minería, Facultad de Ingeniería, Pontificia Universidad Católica de Chile, Santiago, Chile

ARTICLE INFO

*Article history:*
Received 13 December 2011
Received in revised form 22 March 2012
Accepted 16 April 2012
Available online 25 April 2012

*Keywords:*
Laplace equation
Robin boundary condition
Fast multipole algorithm
Boundary element method
Exponential integral function

ABSTRACT

A fast multipole boundary element method (FM-BEM) for solving large-scale potential problems ruled by the Laplace equation in a locally-perturbed 2-D half-plane with a Robin boundary condition is developed in this paper. These problems arise in a wide gamut of applications, being the most relevant one the scattering of water-waves by floating and submerged bodies in water of infinite depth. The method is based on a multipole expansion of an explicit representation of the associated Green's function, which depends on a combination of complex-valued exponential integrals and elementary functions. The resulting method exhibits a computational performance and memory requirements similar to the classic FM-BEM for full-plane potential problems. Numerical examples demonstrate the accuracy and efficiency of the method.

© 2012 Elsevier B.V. All rights reserved.

## 1. Introduction

Robin boundary condition for the Laplace equation is a broadly used mathematical model that arises in a wide gamut of engineering problems. One of the most important applications is the theory of water-waves, in which the Robin boundary condition (with a real parameter) gives a linearized description of the propagation of time-harmonic gravity waves on the surface of an incompressible inviscid irrotational fluid [1,2]. Particularly when considering a compactly perturbed half-plane, this model predicts the scattering of small amplitude water-waves due to the presence of floating or submerged bodies. Otherwise, complex Robin parameters play a role in modeling water-wave phenomena in domains involving porous structures like permeable breakwaters [3]. Other applications include harmonic potentials in domains containing rough surfaces [4], steady-state heat conduction using linear convection boundary conditions [5,6], and approximation of low-frequency sound and electromagnetic wave propagation above the ground [7,8]. More recently this model has been used to simulate the fluid flow induced by nonuniform alternating-current electric fields in electrolytes on microelectrodes [9].

An appropriate approach to numerically solve the Laplace equation above a Robin half-plane is the boundary element method (BEM) [10,11], since it provides a natural framework to take the unboundedness of the computational domain and radiation/decaying conditions at infinity into account. The essence of the BEM is the knowledge of the Green's function of the problem. However, unlike half-plane problems with Dirichlet or Neumann boundary conditions where the Green's function can be directly obtained by applying the method of images, the computation of Green's function for the Robin problem usually entails either the application of the complex image method or Fourier transform techniques that usually lead to complicated non-explicit representations unsuitable for direct numerical evaluations. Expressions for the Green's function of the Laplace equation in two-and three-dimensional Robin half-spaces were first derived by John [12,13]. Since then, many other equivalent expressions have been obtained [1,2,14], based on integrals representations and series expansions. To the authors' knowledge, the first explicit or closed-form expression for the Green's function in the two-dimensional case, was recently derived by Hein et al. [15], by means of a combination of elementary functions and complex-valued exponential integrals. This relatively simple representation can be accurately evaluated numerically in the complex-plane, so it is easy to incorporate it into a BEM code.

An important disadvantage of the conventional BEM is that the discretized boundary integral equation yields a dense system of equations. Therefore, when this method is applied to problems defined in domains with large or complex boundaries where many elements are required, the linear system readily becomes intractable or too expensive to be solved by standard methods. Due to this

* Corresponding author. Current address: Applied & Computational Mathematics, California Institute of Technology, MC 305-16, Pasadena, CA 91125, United States.
*E-mail addresses:* cperezar@caltech.edu (C. Pérez-Arancibia), pramacio@uc.cl (P. Ramaciotti), ricardo.hein@ingmat.com (R. Hein), mduran@ing.uc.cl (M. Durán).

0045-7825/$ - see front matter © 2012 Elsevier B.V. All rights reserved.
http://dx.doi.org/10.1016/j.cma.2012.04.012

reason, conventional BEM has not been considered a practical alternative for large-scale problems [16]. A method for overcoming this drawback is the fast multipole method (FMM) originally introduced by Rokhlin [17] for the Laplace equation in two-dimensions and further developed by Greengard and Rokhlin for the many-body problem [18]. This method allows to speed up the solution of the BEM linear system reducing at the same time data storage requirements. The FMM in conjunction with the BEM and an iterative method for solving the linear system gives rise to the so-called fast multipole boundary element method (FM-BEM). By means of the FMM, time requirements for solving the BEM linear system are reduced to only $\mathcal{O}(N)$ or $\mathcal{O}(N\log N)$ operations, instead of $\mathcal{O}(N^3)$ (direct solver) or $\mathcal{O}(N^2)$ (iterative solver), where $N$ is the number of nodes of the discretized boundary integral equation. This method has been successfully applied to potential problems [19–21], acoustics [22–26], elastostatics [27–29], Stokes flows [30–32], time-harmonic elastodynamics [33,34], and electromagnetic scattering [35–37]. Further references can be found in the comprehensive review article of Nishimura [16] and in the book of Liu [38].

In this article we develop a FM-BEM for solving the Laplace equation in a locally perturbed half-plane with a Robin boundary condition. As it is well-known, the FM-BEM relies on finding an appropriate multipole series for the associated Green's function. Such series was first derived by Ursell [39,40,42], Thorne [41] and Martin [43]. However, the functions upon which Ursell's multipole expansion is expressed are difficult to compute numerically and some of the addition theorems needed to implement the FM-BEM are unknown. In this article we perform a new multipole expansion for the Green's function based on the explicit representation of Hein et al. [15]. Logarithmic terms of the Green's function are expanded as in the classical algorithm, while the terms depending on the exponential integral are expanded in a series of functions that can be computed either directly or by applying simple recurrence relations. Bounds for the truncation error associated to the series are explicitly obtained. We implement an adaptive FM-BEM that exhibits a performance of $\mathcal{O}(N)$ operations per matrix–vector multiplication, the same computational complexity of the original algorithm. The linear system of equations is solved by using the generalized minimal residual (GMRES) algorithm [44]. Numerical examples show the accuracy and efficiency of the proposed algorithm.

The structure of this paper is as follows. In Section 2 we give an overview of the problem, showing its boundary integral equation and its numerical discretization by the collocation BEM. Next, Section 3 deals with the multipole series expansions of the Green's function and of its normal derivative. Subsequently, in Section 4 we describe the algorithm. Finally, in Section 5 we illustrate the use of the method by some examples.

## 2. Robin half-plane problem for the Laplace equation

### 2.1. Problem setup

Let $\Omega_e \subset \mathbb{R}^2_+ = \{(x_1,x_2)\in\mathbb{R}^2 : x_2 > 0\}$ be a locally perturbed half-plane (see Fig. 1) with boundary $\Gamma$ admitting the splitting $\Gamma = \overline{\Gamma_p \cup \Gamma_\infty}$, where $\Gamma_p \cap \Gamma_\infty = \emptyset$, $\Gamma_p \subset \mathbb{R}^2_+$ is bounded, and $\Gamma_\infty \subset \{(x_1,x_2)\in\mathbb{R}^2 : x_2 = 0\}$. Now, we consider the differential problem

$$\begin{cases} \Delta u = 0 & \text{in } \Omega_e, \\ \dfrac{\partial u}{\partial n} - v_s u = f & \text{on } \Gamma, \\ +\text{radiation condition as } |\mathbf{y}| \to +\infty, \end{cases} \tag{1}$$

where the function $v_s : \Gamma \to \mathbb{C}$, $v_s \in L^\infty(\Gamma)$, is referred to as the Robin parameter and is such that

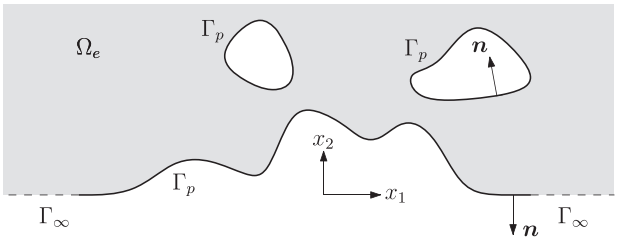


**Fig. 1.** Domain of the Robin half-plane problem.

$$v_s(\mathbf{x}) = v + v_p(\mathbf{x}), \tag{2}$$

with $v\in\mathbb{C}$ being a constant and $v_p : \Gamma \to \mathbb{C}$, $\operatorname{supp}\{v_p\} \subset \Gamma_p$. Due to physical considerations concerning dissipation (cf. [3]), we have that $v$ lies in the first quadrant of the complex plane. More precisely, $0 \leqslant \arg v < \pi/2$. We also assume that the source term $f : \Gamma \to \mathbb{C}, f \in H^{-1/2}(\Gamma)$, is such that $\operatorname{supp}\{f\} \subset \Gamma_p$, which is a standard assumption in the formulation of scattering problems like this, where surface waves are allowed to be diffracted by the perturbation $\Gamma_p$.

In order to perform a boundary integral equation leading to the solution of Eq. (1), we resort to the Green's function given by the solution of the boundary-value problem (cf. [15])

$$\begin{cases} \Delta_{\mathbf{y}} G(\mathbf{x},\mathbf{y}) = \delta_{\mathbf{x}}(\mathbf{y}), & \text{in } \mathbb{R}^2_+, \\ \dfrac{\partial G}{\partial y_2}(\mathbf{x},\mathbf{y}) + vG(\mathbf{x},\mathbf{y}) = 0, & \text{on } \{y_2 = 0\}, \\ +\text{radiation condition as } |\mathbf{y}| \to +\infty, \end{cases} \tag{3}$$

which has to be understood in the sense of distributions on account of the fact that $\delta_{\mathbf{x}} \in \mathcal{D}'(\mathbb{R}^2_+)$ is Dirac's delta distribution supported at $\mathbf{x}\in\mathbb{R}^2_+$. The suitable radiation condition for Eq. (3), which also is the radiation condition for Eq. (1), is given by

$$|G| \leqslant \frac{C}{|\mathbf{y}|} \quad \text{and} \quad \left|\frac{\partial G}{\partial r_{\mathbf{y}}}\right| \leqslant \frac{C}{|\mathbf{y}|^2} \quad \text{if } y_2 > \frac{1}{v}\ln(1+v\pi|\mathbf{y}|), \tag{4a}$$

$$|G| \leqslant C \quad \text{and} \quad \left|\frac{\partial G}{\partial r_{\mathbf{y}}} - \mathrm{i}vG\right| \leqslant \frac{C}{|\mathbf{y}|} \quad \text{if } y_2 < \frac{1}{v}\ln(1+v\pi|\mathbf{y}|). \tag{4b}$$

It qualitatively corresponds to surface waves propagating along the flat boundary $\Gamma_\infty$ going away from the fixed point $\mathbf{x}\in\mathbb{R}^2_+$. According to [15], problem Eq. (3) admits a unique explicit solution

$$\begin{aligned} G(\mathbf{x},\mathbf{y}) = {} & \frac{1}{2\pi}\ln|\mathbf{y}-\mathbf{x}| - \frac{1}{2\pi}\ln|\mathbf{y}-\overline{\mathbf{x}}| - \mathrm{i}\mathrm{e}^{-v(y_2+x_2)}\cos(v(y_1-x_1)) \\ & + \frac{\mathrm{e}^{-v(y_2+x_2)}}{2\pi}\left\{\mathrm{e}^{\mathrm{i}v(y_1-x_1)}\mathrm{Ei}(v((y_2+x_2)-\mathrm{i}(y_1-x_1))) \right. \\ & \left. + \mathrm{e}^{-\mathrm{i}v(y_1-x_1)}\mathrm{Ei}(v((y_2+x_2)+\mathrm{i}(y_1-x_1)))\right\}, \end{aligned} \tag{5}$$

where $\overline{\mathbf{x}} = (x_1,-x_2)$ is the image point of $\mathbf{x}$ and where Ei denotes the exponential integral function (cf. [45]) defined as the Cauchy principal-value integral

$$\mathrm{Ei}(z) = -\int_{-\infty}^{z}\frac{\mathrm{e}^t}{t}\mathrm{d}t, \quad |\arg z| < \pi. \tag{6}$$

Likewise, the gradient of Eq. (5) can be explicitly computed and is given by

$$\begin{aligned} \nabla_{\mathbf{y}} G(\mathbf{x},\mathbf{y}) = {} & \frac{\mathbf{y}-\mathbf{x}}{2\pi|\mathbf{y}-\mathbf{x}|^2} + \frac{\mathbf{y}-\overline{\mathbf{x}}}{2\pi|\mathbf{y}-\overline{\mathbf{x}}|^2} - \mathrm{i}v\mathrm{e}^{-v(y_2+x_2)}\begin{bmatrix}\sin(v(y_1-x_1))\\ \cos(v(y_1-x_1))\end{bmatrix} \\ & - \frac{v}{2\pi}\mathrm{e}^{-v(y_2+x_2)}\left\{\begin{bmatrix}-\mathrm{i}\\ 1\end{bmatrix}\mathrm{e}^{\mathrm{i}v(y_1-x_1)}\mathrm{Ei}(v((y_2+x_2)-\mathrm{i}(y_1-x_1))) \right. \\ & \left. + \begin{bmatrix}\mathrm{i}\\ 1\end{bmatrix}\mathrm{e}^{-\mathrm{i}v(y_1-x_1)}\mathrm{Ei}(v((y_2+x_2)+\mathrm{i}(y_1-x_1)))\right\} \end{aligned} \tag{7}$$

Thanks to the Green's function Eq. (5), it is possible to derive an integral representation and a boundary integral equation for the solution of Eq. (1). They respectively read as follows,

$$u(\mathbf{x}) = \int_{\Gamma_p} K(\mathbf{x},\mathbf{y})u(\mathbf{y})\mathrm{d}\gamma(\mathbf{y}) + \int_{\Gamma_p} G(\mathbf{x},\mathbf{y})f(\mathbf{y})\mathrm{d}\gamma(\mathbf{y}), \quad \mathbf{x}\in\Omega_e\cup\Gamma_\infty, \tag{8}$$

$$\frac{u(\mathbf{x})}{2} = \int_{\Gamma_p} K(\mathbf{x},\mathbf{y})u(\mathbf{y})\mathrm{d}\gamma(\mathbf{y}) + \int_{\Gamma_p} G(\mathbf{x},\mathbf{y})f(\mathbf{y})\mathrm{d}\gamma(\mathbf{y}), \quad \mathbf{x}\in\Gamma_p, \tag{9}$$

where we have introduced an additional integral kernel defined by

$$K(\mathbf{x},\mathbf{y}) \stackrel{\text{def}}{=} \frac{\partial G}{\partial n_{\mathbf{y}}}(\mathbf{x},\mathbf{y}) - v_s(\mathbf{y})G(\mathbf{x},\mathbf{y}), \quad \mathbf{x}\in\Omega_e\cup\Gamma, \quad \mathbf{y}\in\Gamma. \tag{10}$$

Results on the existence and uniqueness of solutions (for a restricted set of Robin parameters) for the boundary integral Eq. (9) can be found in [46], whereas explicit examples of non-uniqueness can be found in [47] and references therein.

It has to be pointed out that the restriction on the domain $\Omega_e$ to lie on the upper half-plane $\mathbb{R}^2_+$ stems from the fact that formulae Eqs. (8) and (9) are only valid in this case. If a perturbation towards the lower half-plane is desired for $\Omega_e$, then the derivation of an appropriate integral representation and equation requires the consideration of the additional singularities of the Green's function in the complementary half-space, i.e., the logarithmic singularity at the image point $\overline{\mathbf{x}}$ and the jump of the $y_1$-derivative across the half-line $\Upsilon = \{y_1 = x_1, y_2 < -x_2\}$ due to the effect of the analytic branch cut of the complex-valued exponential integral. Both singularities yield Dirac mass distributions when the Laplacian of the Green's function is computed (cf. [15,46]). Despite the fact that this restriction may appear unphysical and stringent for some applications, it is fulfilled by a wide variety of problems involving linearized water-waves, where the perturbation models submerged and floating objects, and where the water body remains always contained inside the considered half-plane.

### 2.2. Discretization of the boundary integral equation

In what follows we are interested in numerically solving Eq. (9) by combining the BEM and the FMM. For the sake of efficiency and simplicity, we discretize Eq. (9) through a colocation method because this approach requires quadrature approximation of single boundary integrals, while, for instance, the variational Galerkin approach requires the evaluation of double boundary integrals. Nevertheless, minor modifications of this FM-BEM make it possible to apply it within a variational Galerkin approach as well.

Let us assume that $\Gamma_p = \bigcup_{\ell=1}^N \Gamma_\ell$, where $\Gamma_{\ell_1}\cap\Gamma_{\ell_2} = \emptyset$ if $\ell_1 \neq \ell_2$, and that each $\Gamma_\ell$ is a straight line segment in the plane. We look then for an approximation of the form

$$u(\mathbf{y}) \approx u_h(\mathbf{x}) = \sum_{j=1}^N u_j\varphi_j(\mathbf{y}), \tag{11}$$

where the (standard) basis functions $\varphi_j(\mathbf{y})$, $j = 1,\ldots,N$, are defined on $\Gamma_p$ and satisfy $\varphi_j(\mathbf{x}_i) = \delta_{ij}$ with $\mathbf{x}_i$, $i = 1,\ldots,N$, being the collocation points. Here, the approximate solution $u_h$ depends on the discretization refinement $h$, defined as $h = \max_{\ell\in\{1,\ldots,N\}}|\Gamma_\ell|$.

In order to obtain a system of equations for the coefficients $u_j$ in Eq. (11) we substitute the right-hand side of Eq. (11) into Eq. (9) and evaluate the terms in this equation at the collocation points. It yields the system of equations

$$\left(\frac{\boldsymbol{I}}{2} - \boldsymbol{K}\right)\mathbf{u} = \mathbf{G}\mathbf{f}, \tag{12}$$

where $f_i = f(\mathbf{x}_i)$, $\boldsymbol{I}\in\mathbb{C}^{N\times N}$ is the identity matrix, and

$$k_{ij} \stackrel{\text{def}}{=} \sum_{\ell=1}^N \int_{\Gamma_\ell} K(\mathbf{x}_i,\mathbf{y})\varphi_j(\mathbf{y})\mathrm{d}\gamma(\mathbf{y}), \quad i,j = 1,\ldots,N, \tag{13}$$

$$g_{ij} \stackrel{\text{def}}{=} \sum_{\ell=1}^N \int_{\Gamma_\ell} G(\mathbf{x}_i,\mathbf{y})\varphi_j(\mathbf{y})\mathrm{d}\gamma(\mathbf{y}), \quad i,j = 1,\ldots,N. \tag{14}$$

As should be expected in a collocation BEM $\boldsymbol{K}\in\mathbb{C}^{N\times N}$ is a general dense non-symmetric matrix, thus $\mathcal{O}(N^2)$ operations are needed to compute its coefficients. It is important to observe that due to the form of the Green's function Eq. (5), the computational complexity to compute $\boldsymbol{K}$ is about ten times the one required to compute the discretization matrix (with the same number of degrees of freedom) associated to the potential problem of a bounded obstacle in the whole plane, such as the one studied in [21].

The linear system Eq. (12) can be solved by direct methods like the LU decomposition and the Gauss elimination algorithm. However, those methods are considered inefficient for problems having a large number of degrees of freedom $N$ due to the fact that $\mathcal{O}(N^3)$ operations are required. On the other hand, iterative methods like, e.g., the conjugate gradient or GMRES algorithm, perform considerably better than direct solvers when $\boldsymbol{I}/2 - \boldsymbol{K}$ is well conditioned. Nevertheless, those methods entail evaluating several times the multiplication of $\boldsymbol{K}$ by a complex vector, which is also considered inefficient for large $N$ because it demands $\mathcal{O}(N^2)$ operations per iteration.

The key idea of the FM-BEM is to speed up the matrix–vector multiplications required by iterative linear system solvers to converge within a prescribed tolerance, reducing its complexity to only $\mathcal{O}(N)$ operations per iteration. To do so, matrix $\boldsymbol{K}$ must be interpreted as the sum of two matrices, namely $\boldsymbol{K}^{nf}$ and $\boldsymbol{K}^{ff}$, where $\boldsymbol{K}^{nf}$ is due to the contribution of sources located in the near field, and $\boldsymbol{K}^{ff}$ is due to the contributions of sources located in the far field. The exact meaning of the near and far field will be established later on this paper. The entries of $\boldsymbol{K}^{nf}$ are explicitly computed as in the conventional BEM, i.e., the singularities of $K$ in the integral Eq. (13) are solved analytically while the remaining terms are computed employing an accurate quadrature rule (see [46]). If enough memory is available, $\boldsymbol{K}^{nf}$ is stored, so it is not necessary to recompute it in subsequent iterations. By contrast, the entries of $\boldsymbol{K}^{ff}$ are never explicitly computed. Instead, in each solver iteration the result of the matrix multiplication between $\boldsymbol{K}^{ff}$ and a vector $\boldsymbol{v}$ is efficiently approximated by using a multipole expansion for $\int_{\Gamma_\ell} K(\mathbf{x}_i,\mathbf{y})\varphi_j(\mathbf{y})\ v_j\mathrm{d}\gamma(\mathbf{y})$. The next sections address the issue of describing how this multipole expansion is applied to accelerate the solution of the problem, reducing at the same time the memory requirements.

## 3. Series expansions

In this section we perform a series representation of the Green's function and its normal derivative in order to derive the multipole and local expansions.

### 3.1. Complex variable notation

As is conventional in two-dimensional potential problems, we resort to the use of complex analysis tools. Thus, let us consider the bijective map $\mathbb{R}^2_+\times\mathbb{R}^2_+ \ni (\mathbf{x},\mathbf{y}) \mapsto (w,z)\in\mathbb{C}_+\times\mathbb{C}_+$, defined by $w(\mathbf{x}) = x_1 + \mathrm{i}x_2$ and $z(\mathbf{y}) = y_1 + \mathrm{i}y_2$, where $\mathbb{C}_+ = \{z\in\mathbb{C} : \Im\mathrm{m}\, z > 0\}$. This map allows to express Eq. (5) as

$$\begin{aligned} \mathrm{G}(w,z) = {} & \frac{1}{2\pi}\Re\mathrm{e}\{\ln(w-z) - \ln(\overline{w}-z)\} \\ & - \frac{\mathrm{i}}{2}\left\{\mathrm{e}^{-\mathrm{i}\nu(\overline{w}-z)} + \mathrm{e}^{\mathrm{i}\nu(w-\overline{z})}\right\} + \frac{\mathrm{e}^{-\mathrm{i}\nu(\overline{w}-z)}}{2\pi}\mathrm{Ei}(\mathrm{i}\nu(\overline{w}-z)) \\ & + \frac{\mathrm{e}^{-\mathrm{i}\nu(\overline{z}-w)}}{2\pi}\mathrm{Ei}(\mathrm{i}\nu(\overline{z}-w)), \end{aligned} \tag{15}$$

where $G(\mathbf{x},\mathbf{y}) = \mathrm{G}(w(\mathbf{x}), z(\mathbf{y}))$. Here, the complex logarithm and the exponential integral function have to be understood in the sense of the principal value, so their domain of definition is restricted to $0 < |\arg z| < \pi$. Likewise, we get that the normal derivative of the Green's function can be expressed as

$$\mathrm{F}(w,z) = \frac{1}{2\pi}\Re\mathrm{e}\left\{\frac{\eta}{z-w}+\frac{\eta}{z-\overline{w}}\right\}+\frac{v}{2}\left\{\eta\mathrm{e}^{-\mathrm{i}v(\overline{w}-z)}-\overline{\eta}\mathrm{e}^{\mathrm{i}v(w-\bar{z})}\right\} + \frac{\mathrm{i}v}{2\pi}\left\{\eta\mathrm{e}^{-\mathrm{i}v(\overline{w}-z)}\mathrm{Ei}(\mathrm{i}v(\overline{w}-z))-\overline{\eta}\mathrm{e}^{-\mathrm{i}v(\bar{z}-w)}\mathrm{Ei}(\mathrm{i}v(\bar{z}-w))\right\}, \tag{16}$$

where $\partial G(\mathbf{x}(w),\mathbf{y}(z))/\partial n_{\mathbf{y}} = \mathrm{F}(w,z)$ and $\eta(z) = \eta_1(\mathbf{y}(z)) + \mathrm{i}\eta_2(\mathbf{y}(z))$ with $n_{\mathbf{y}} = [\eta_1,\eta_2]^T$ being the unit normal vector pointing outwards from the region $\Omega_e$. Identity Eq. (16) follows directly by taking the dot product between $n_{\mathbf{y}}$ and the Green's function's gradient Eq. (7) and by transforming the resulting expression into complex variable notation.

### 3.2. Series expansion of the logarithmic terms

We start by expanding the logarithmic terms of the Green's functions. Thus, let $z$ and $w \in \mathbb{C}_+$ such that $|z| < |w|$. Then, resorting to some well-known results for the Laplace equation in the plane (cf. [17,18,49]), we get that all terms in Eq. (15) involving logarithms can be expanded as

$$\ln(w-z) = -\sum_{n=0}^{\infty}\mathrm{S}_n^{(1)}(w)\mathrm{R}_n^{(1)}(z), \quad |z| < |w|, \tag{17}$$

where the functions used to perform the series Eq. (17) are defined as

$$\mathrm{R}_n^{(1)}(z) \overset{\text{def}}{=} \frac{z^n}{n!}, \quad n \geqslant 0, \tag{18a}$$

$$\mathrm{S}_n^{(1)}(z) \overset{\text{def}}{=} \frac{(n-1)!}{z^n}, \quad n \geqslant 1; \quad \text{and } \mathrm{S}_0^{(1)}(z) \overset{\text{def}}{=} -\ln(z). \tag{18b}$$

An addition formula for the functions $\mathrm{R}_n^{(1)}$ can be readily obtained from the binomial theorem, and its given by

$$\mathrm{R}_n^{(1)}(z_1+z_2) = \sum_{m=0}^{n}\mathrm{R}_{n-m}^{(1)}(z_1)\mathrm{R}_m^{(1)}(z_2). \tag{19}$$

Likewise, an analogous result for the functions $\mathrm{S}_n^{(1)}$ is

$$\mathrm{S}_n^{(1)}(z_1+z_2) = \sum_{m=0}^{\infty}\mathrm{S}_{n+m}^{(1)}(z_1)\mathrm{R}_m^{(1)}(-z_2), \quad |z_2| < |z_1|, \tag{20}$$

which can be worked out by computing the Laurent series expansion of $\mathrm{S}^{(1)}(z_1+z_2)$ about $z_2$ when $|z_2| < |z_1|$.

### 3.3. Series expansion of the exponential integral function

Now we deal with the series expansion of the Green's function terms depending on the exponential integral function, which is based on the next two propositions.

**Proposition 3.1** (see [50]). *Let $z \in \mathbb{C}\setminus\{0\}$ such that $|\arg z| < \pi$. Thus, the derivatives of the exponential integral function at $z$ are given by*

$$\frac{\mathrm{d}^n\mathrm{Ei}}{\mathrm{d}z^n}(z) = d_{n-1}(z), \quad n \geqslant 1, \tag{21}$$

*where the functions $d_n$ are defined as*

$$d_n(z) = \frac{\mathrm{d}^n}{\mathrm{d}z^n}\left(\frac{\mathrm{e}^z}{z}\right), \quad n \geqslant 0$$

*and can be computed through the recurrence relation*

$$d_n(z) + \frac{n}{z}d_{n-1}(z) = \frac{\mathrm{e}^z}{z}. \tag{22}$$

*Furthermore, the functions $d_n$ can be explicitly expressed as*

$$d_n(z) = (-1)^n\frac{n!}{z^{n+1}}\mathrm{e}^z\sum_{k=0}^{n}\frac{(-z)^k}{k!}, \quad n \geqslant 0. \tag{23}$$

The next proposition establishes a series representation of the exponential integral function.

**Proposition 3.2.** *Let $v \in \mathbb{C}$ such that $0 \leqslant \arg v \leqslant \pi/2$. Then, the Taylor series expansion*

$$\mathrm{Ei}(\mathrm{i}v(\overline{w}-z)) = \mathrm{Ei}(\mathrm{i}v\overline{w}) + \sum_{n=1}^{\infty}\frac{d_{n-1}(\mathrm{i}v\overline{w})}{n!}(-\mathrm{i}vz)^n \tag{24}$$

*holds true for all complex numbers $z$ and $w$ belonging to $\mathbb{C}_+$ such that $|z| < |\overline{w}|$.*

**Proof.** First we observe that the exponential integral is a single-valued function in the region $|\arg z| < \pi$, so the function $\mathrm{Ei}(\mathrm{i}v\overline{w})$ is single-valued for all $w \in \mathbb{C}_+$ due to the fact that $-\pi/2 < \arg\{\mathrm{i}v\overline{w}\} < \pi$ when $v$ lies in the first quadrant. Thus, as the exponential integral is also analytic in that region, we are allowed to perform a Taylor series about $\mathrm{i}v\overline{w}$ to get Eq. (24), which is valid for all $z \in \mathbb{C}_+$ such that $|vz| < \rho$, with $\rho$ being the radius of convergence of the series. Now, as it is well known (cf. [51]), $\rho$ can be determined by

$$\rho = \lim_{n\to\infty}\left|\frac{d_{n-1}(\mathrm{i}v\overline{w})/n!}{d_n(\mathrm{i}v\overline{w})/(n+1)!}\right| = |v||\overline{w}|\lim_{n\to\infty}\left\{\left(\frac{n+1}{n}\right)\frac{\left|\sum_{k=0}^{n-1}\frac{(\mathrm{i}v\overline{w})^k}{k!}\right|}{\left|\sum_{k=0}^{n}\frac{(\mathrm{i}v\overline{w})^k}{k!}\right|}\right\},$$

where the last term follows from Eq. (23). Then, taking into account that

$$\lim_{n\to\infty}\sum_{k=0}^{n-1}\frac{(\mathrm{i}v\overline{w})^k}{k!} = \lim_{n\to\infty}\sum_{k=0}^{n}\frac{(\mathrm{i}v\overline{w})^k}{k!} = \mathrm{e}^{\mathrm{i}v\overline{w}},$$

we get that $\rho = |v\overline{w}|$. Using this fact it can be concluded that the series Eq. (24) is valid for all $z$ and $w \in \mathbb{C}_+$ such that $|z| < |\overline{w}|$. □

In order to write in a convenient form the series expansion of the Green's function terms depending on the exponential integral, we define the sets of functions

$$\mathrm{R}_n^{(2)}(z) \overset{\text{def}}{=} \frac{\mathrm{e}^{\mathrm{i}vz}(\mathrm{i}vz)^n}{n!}, \quad n \geqslant 0, \tag{25}$$

$$\mathrm{S}_n^{(2)}(z) \overset{\text{def}}{=} \begin{cases} \mathrm{e}^{-\mathrm{i}vz}\mathrm{Ei}(\mathrm{i}vz) & \text{if } n = 0, \\ (-1)^n\mathrm{e}^{-\mathrm{i}vz}d_{n-1}(\mathrm{i}vz) = -\dfrac{(n-1)!}{(\mathrm{i}vz)^n}\displaystyle\sum_{k=0}^{n-1}\frac{(-\mathrm{i}vz)^k}{k!} & \text{if } n \geqslant 1, \end{cases} \tag{26}$$

where the functions $d_n$ are defined in Eq. (22). Let us observe that henceforth the functions $\mathrm{R}_n^{(2)}$ and $\mathrm{S}_n^{(2)}$ depend implicitly on the impedance parameter $v$. By using these functions we achieve that

$$\mathrm{e}^{-\mathrm{i}v(\overline{w}-z)}\mathrm{Ei}(\mathrm{i}v(\overline{w}-z)) = \sum_{n=0}^{\infty}\mathrm{S}_n^{(2)}(\overline{w})\mathrm{R}_n^{(2)}(z), \quad |z| < |\overline{w}|, \tag{27a}$$

$$\mathrm{e}^{-\mathrm{i}v(\bar{z}-w)}\mathrm{Ei}(\mathrm{i}v(\bar{z}-w)) = \sum_{n=0}^{\infty}\mathrm{S}_n^{(2)}(-w)\mathrm{R}_n^{(2)}(-\bar{z}), \quad |z| < |\overline{w}|. \tag{27b}$$

It can be straightforwardly deduced from Eq. (19) that the functions $\mathrm{R}_n^{(2)}$ satisfy the addition formula

$$\mathrm{R}_n^{(2)}(z_1+z_2) = \sum_{m=0}^{n}\mathrm{R}_{n-m}^{(2)}(z_1)\mathrm{R}_m^{(2)}(z_2), \quad n \geqslant 0. \tag{28}$$

On the other hand, as the functions $\mathrm{S}_n^{(2)}$ are, up to the factor $\mathrm{e}^{-vz}$, the derivatives of the exponential integral and are analytical in $\mathbb{C}\setminus\{0\}$

when $n \geqslant 1$, we get from the Taylor theorem that they satisfy the addition formula

$$\mathrm{S}_n^{(2)}(z_1+z_2)=\sum_{m=0}^{\infty}\mathrm{S}_{n+m}^{(2)}(z_2)\mathrm{R}_m^{(2)}(-z_1),\quad n\geqslant 1,\quad |z_1|<|z_2|. \tag{29}$$

Formula Eq. (29) can be proved by resorting to the same arguments used in the proof of Proposition 3.2.

### 3.4. Expansion of the Green's function

Now we are in position to perform the series representation of the Green's function Eq. (15) and its normal derivative Eq. (16). Let $z$ and $w\in\mathbb{C}_+$ such that $|z|<|w|$. Then, by directly using Eqs. (17) and (27a) we get that the Green's function admits the series expansion

$$\begin{aligned}\mathrm{G}(w,z)=&\frac{1}{2\pi}\sum_{n=0}^{\infty}\Re\mathrm{e}\Big\{\Big[\mathrm{S}_n^{(1)}(\overline{w})-\mathrm{S}_n^{(1)}(w)\Big]\mathrm{R}_n^{(1)}(z)\Big\}\\&+\frac{1}{2\pi}\sum_{n=0}^{\infty}\Big\{\mathrm{S}_n^{(2)}(\overline{w})\mathrm{R}_n^{(2)}(z)+\mathrm{S}_n^{(2)}(-w)\mathrm{R}_n^{(2)}(-\overline{z})\Big\}\\&-\frac{\mathrm{i}}{2}\Big\{\mathrm{e}^{-\mathrm{i}v\overline{w}}\mathrm{R}_0^{(2)}(z)+\mathrm{e}^{\mathrm{i}vw}\mathrm{R}_0^{(2)}(-\overline{z})\Big\}.\end{aligned} \tag{30}$$

To perform an expansion of the normal derivative we take the derivative of Eq. (30). In order to do so we first note that the Green's function can be expressed as $\mathrm{G}(w,z)=f_1(z)+f_2(\overline{z})$ where $f_1$ and $f_2$ are analytic functions of $z\in\mathbb{C}_+$ and $\overline{z}\in\mathbb{C}_-$ respectively. Consequently, it can be deduced that its gradient can be computed as $\big[f_1'(z)+f_2'(\overline{z}),\mathrm{i}f_1'(z)-\mathrm{i}f_2'(\overline{z})\big]$ and, consequently, its normal derivative is given by $\mathrm{F}(w,z)=\eta f_1'(z)+\overline{\eta}f_2'(\overline{z})$. Recognizing the function $f_1$ and $f_2$ in Eq. (30) and applying the previous formula, we achieve that

$$\begin{aligned}\mathrm{F}(w,z)=&\frac{1}{2\pi}\sum_{n=0}^{\infty}\Re\mathrm{e}\Big\{\eta\Big[\mathrm{S}_n^{(1)}(\overline{w})-\mathrm{S}_n^{(1)}(w)\Big]\mathrm{R}_n^{(1)\prime}(z)\Big\}\\&+\frac{1}{2\pi}\sum_{n=0}^{\infty}\Big\{\eta\mathrm{S}_n^{(2)}(\overline{w})\mathrm{R}_n^{(2)\prime}(z)-\overline{\eta}\mathrm{S}_n^{(2)}(-w)\mathrm{R}_n^{(2)\prime}(-\overline{z})\Big\}\\&-\frac{\mathrm{i}}{2}\Big\{\eta\mathrm{e}^{-\mathrm{i}v\overline{w}}\mathrm{R}_0^{(2)\prime}(z)-\overline{\eta}\mathrm{e}^{\mathrm{i}vw}\mathrm{R}_0^{(2)\prime}(-\overline{z})\Big\}.\end{aligned} \tag{31}$$

Here, the derivative of the functions $\mathrm{R}_n^{(1)}$, $j=1,2$, can be computed through the formulae

$$\begin{aligned}&\mathrm{R}_0^{(1)\prime}(z)=0,\quad \mathrm{R}_0^{(2)\prime}(z)=\mathrm{i}v\mathrm{R}_0^{(2)}(z),\quad \mathrm{R}_n^{(1)\prime}(z)=\mathrm{R}_{n-1}^{(1)}(z),\\&\mathrm{R}_n^{(2)\prime}(z)=\mathrm{i}v\Big\{\mathrm{R}_n^{(2)}(z)+\mathrm{R}_{n-1}^{(2)}(z)\Big\},\quad n\geqslant 1.\end{aligned} \tag{32}$$

It can be directly checked that the addition formulae Eq. (19) and Eq. (28) are as well accomplished by the derivatives, i.e.,

$$\mathrm{R}_n^{(j)\prime}(z_1+z_2)=\sum_{m=0}^{n}\mathrm{R}_{n-m}^{(j)}(z_1)\mathrm{R}_m^{(j)\prime}(z_2),\quad n\geqslant 0,\ j=1,2. \tag{33}$$

## 4. Fast multipole boundary element method

In this section we develop the multipole and local expansions of the Green's function for the Laplace equation in an impedance half-plane and its application to the FM-BEM.

### 4.1. Multipole expansion, moments definition and moment-to-moment translation

We start by deducing the multipole expansion of integrals of the form Eq. (13). Accordingly, let us define $\mathrm{K}(w,z)=K(\mathbf{x}(w),\mathbf{y}(z))$ with $K$ defined in Eq. (10), and consider $\Gamma_p$ to be a curve in $\mathbb{C}_+$. Now, we take $z_0\in\mathbb{C}_+$ such that $|z-z_0|<r$ for all $z\in\Gamma_\ell\subset\Gamma_p$ with $r>0$, and we let $w\in\mathbb{C}_+$ be such that $r<|w-z_0|\leqslant|\overline{w}-z_0|$. Thus, combining Eqs. (30) and (31) we can establish the multipole series expansion

$$\begin{aligned}\int_{\Gamma_\ell}\mathrm{K}(w,z)\varphi(z)\mathrm{d}\sigma_z=&\frac{1}{4\pi}\sum_{n=0}^{\infty}\Big\{\mathrm{S}_n^{(1)}(\overline{w}-z_0)-\mathrm{S}_n^{(1)}(w-z_0)\Big\}\mathrm{M}_{n,\ell}^{(1)}(z_0)\\&+\frac{1}{4\pi}\sum_{n=0}^{\infty}\Big\{\mathrm{S}_n^{(1)}(w-\overline{z}_0)-\mathrm{S}_n^{(1)}(\overline{w-z_0})\Big\}\widehat{\mathrm{M}}_{n,\ell}^{(1)}(z_0)\\&+\frac{1}{2\pi}\sum_{n=0}^{\infty}\Big\{\mathrm{S}_n^{(2)}(\overline{w}-z_0)\mathrm{M}_{n,\ell}^{(2)}(z_0)+\mathrm{S}_n^{(2)}(\overline{z}_0-w)\widehat{\mathrm{M}}_{n,\ell}^{(2)}(z_0)\Big\}\\&-\frac{\mathrm{i}}{2}\Big\{\mathrm{e}^{-\mathrm{i}v(\overline{w}-z_0)}\mathrm{M}_{0,\ell}^{(2)}(z_0)+\mathrm{e}^{-\mathrm{i}v(\overline{z}_0-w)}\widehat{\mathrm{M}}_{0,\ell}^{(2)}(z_0)\Big\},\end{aligned} \tag{34}$$

where the multipole moments about the point $z_0$ are defined as

$$\mathrm{M}_{n,\ell}^{(i)}(z_0)\overset{\text{def}}{=}\begin{cases}\displaystyle\int_{\Gamma_\ell}\Big[\eta\mathrm{R}_n^{(1)\prime}(z-z_0)-v_s(z)\mathrm{R}_n^{(1)}(z-z_0)\Big]\varphi(z)\mathrm{d}\sigma_z,\ i=1,\\ \displaystyle\int_{\Gamma_\ell}\Big[\eta\mathrm{R}_n^{(2)\prime}(z-z_0)-v_s(z)\mathrm{R}_n^{(2)}(z-z_0)\Big]\varphi(z)\mathrm{d}\sigma_z,\ i=2,\end{cases} \tag{35}$$

$$\widehat{\mathrm{M}}_{n,\ell}^{(i)}(z_0)\overset{\text{def}}{=}\begin{cases}\displaystyle\int_{\Gamma_\ell}\Big[\overline{\eta}\mathrm{R}_n^{(1)\prime}(\overline{z-z_0})-v_s(z)\mathrm{R}_n^{(1)}(\overline{z-z_0})\Big]\varphi(z)\mathrm{d}\sigma_z,\quad i=1,\\ \displaystyle\int_{\Gamma_\ell}\Big[-\overline{\eta}\mathrm{R}_n^{(2)\prime}(\overline{z_0-z})-v_s(z)\mathrm{R}_n^{(2)}(\overline{z_0-z})\Big]\varphi(z)\mathrm{d}\sigma_z,\ i=2.\end{cases} \tag{36}$$

Let us observe that when $v_s$ is a piecewise constant function on the segments $\Gamma_\ell$, the moments can be computed analytically for a wide range of nodal basis functions $\varphi_j$.

At this stage it should be added that the multipole expansion Eq. (34) is also valid to evaluate the integrals $\int_{\Gamma_\ell}\mathrm{G}(w,z)\varphi(z)\mathrm{d}\sigma_z$ and $\int_{\Gamma_\ell}\mathrm{F}(w,z)\varphi(z)\mathrm{d}\sigma_z$ when the moments, Eqs. (35) and (36), are computed by replacing $\eta=0$ and $v_s=-1$ in the case of the integral involving the kernel G, and replacing $v_s=0$ in the case of the integral involving the kernel F.

A key issue for the efficiency of the FM-BEM is to find a way to shift the moments from $z_0$ to a new nearby point $z_{0'}$. To do so, we replace $z_0$ by $z_{0'}$ in Eqs. (35) and (36), and write $z-z_{0'}=z_1+z_2$, with $z_1=z-z_0$ and $z_2=z_0-z_{0'}$. Therefore, applying the addition formulae Eqs. (19), (28), and (33), we get that the moments about $z_{0'}$ can expressed as a linear combination of the moments about $z_0$. More precisely, this procedure yields the formulae

$$\mathrm{M}_{n,\ell}^{(i)}(z_{0'})=\begin{cases}\displaystyle\sum_{m=0}^{n}\mathrm{R}_{n-m}^{(1)}(z_0-z_{0'})\mathrm{M}_{m,\ell}^{(1)}(z_0),\quad i=1,\\ \displaystyle\sum_{m=0}^{n}\mathrm{R}_{n-m}^{(2)}(z_0-z_{0'})\mathrm{M}_{m,\ell}^{(2)}(z_0),\quad i=2,\end{cases} \tag{37}$$

$$\widehat{\mathrm{M}}_{n,\ell}^{(i)}(z_{0'})=\begin{cases}\displaystyle\sum_{m=0}^{n}\mathrm{R}_{n-m}^{(1)}(\overline{z_0-z_{0'}})\widehat{\mathrm{M}}_{m,\ell}^{(1)}(z_0),\quad i=1,\\ \displaystyle\sum_{m=0}^{n}\mathrm{R}_{n-m}^{(2)}(\overline{z_{0'}-z_0})\widehat{\mathrm{M}}_{m,\ell}^{(2)}(z_0),\quad i=2\end{cases} \tag{38}$$

referred to as moment-to-moment (M2M) translations.

### 4.2. Moment-to-local and local-to-local translations

Let $w_0\in\mathbb{C}_+$ be such that $|w-w_0|<r<|w_0-z_0|\leqslant|\overline{w}_0-z_0|$ and let us introduce the auxiliary variables $z_2=w_0-z_0$, $z_3=\overline{w}_0-z_0$ and $z_1=w-w_0$. Expressing Eq. (34) using these new variables we get

$$\begin{aligned}\int_{\Gamma_\ell}\mathrm{K}(w,z)\varphi(z)\mathrm{d}\sigma_z=&\frac{1}{4\pi}\sum_{n=0}^{\infty}\Big[\mathrm{S}_n^{(1)}(\overline{z}_1+z_3)-\mathrm{S}_n^{(1)}(z_1+z_2)\Big]\mathrm{M}_{n,\ell}^{(1)}(z_0)\\&+\frac{1}{4\pi}\sum_{n=0}^{\infty}\Big[\mathrm{S}_n^{(1)}(z_1+\overline{z_3})-\mathrm{S}_n^{(1)}(\overline{z_1+z_2})\Big]\widehat{\mathrm{M}}_{n,\ell}^{(1)}(z_0)\\&+\frac{1}{2\pi}\sum_{n=0}^{\infty}\Big\{\mathrm{S}_n^{(2)}(\overline{z}_1+z_3)\mathrm{M}_{n,\ell}^{(2)}(z_0)+\mathrm{S}_n^{(2)}(-z_1-\overline{z_3})\widehat{\mathrm{M}}_{n,\ell}^{(2)}(z_0)\Big\}\\&-\frac{\mathrm{i}}{2}\Big\{\mathrm{e}^{-\mathrm{i}v(\overline{z}_1+z_3)}\mathrm{M}_{0,\ell}^{(2)}(z_0)+\mathrm{e}^{\mathrm{i}v(z_1+\overline{z_3})}\widehat{\mathrm{M}}_{0,\ell}^{(2)}(z_0)\Big\}.\end{aligned}$$

Subsequently, applying addition formulae Eqs. (20) and (29) to expand the functions $S_n^{(i)}$, $i=1,2$, and rewriting the resulting expression as a function of the original variables $z_0, w$ and $w_0$, we achieve that

$$\begin{aligned}\int_{\Gamma_\ell} K(w,z)\varphi(z)d\sigma_z = &\frac{1}{4\pi}\sum_{m=0}^{\infty} R_m^{(1)}(\overline{w_0-w})\left\{L_{m,\ell}^{(1)}(\overline{w}_0)-\widehat{L}_{m,\ell}^{(1)}(w_0)\right\}\\ &+\frac{1}{4\pi}\sum_{m=0}^{\infty} R_m^{(1)}(w_0-w)\left\{\widehat{L}_{m,\ell}^{(1)}(\overline{w}_0)-L_{m,\ell}^{(1)}(w_0)\right\}\\ &+\frac{1}{2\pi}\sum_{m=0}^{\infty} R_m^{(2)}(\overline{w_0-w})L_{m,\ell}^{(2)}(\overline{w}_0)+R_m^{(2)}(w-w_0)\widehat{L}_{m,\ell}^{(2)}(\overline{w}_0)\\ &-\frac{i}{2}\left\{R_0^{(2)}(\overline{w_0-w})L_{0,\ell}^{(3)}(\overline{w}_0)+R_0^{(2)}(w-w_0)\widehat{L}_{0,\ell}^{(3)}(\overline{w}_0)\right\},\end{aligned} \tag{39}$$

where we introduced the local expansions coefficients $L_{m,\ell}^{(i)}$ and $\widehat{L}_{m,\ell}^{(i)}$, $i=1,2,3$, respectively defined as

$$L_{m,\ell}^{(i)}(w_0)\overset{\text{def}}{=}\begin{cases}\displaystyle\sum_{n=0}^{\infty} S_{n+m}^{(1)}(w_0-z_0)M_{n,\ell}^{(1)}(z_0), & i=1,\\ \displaystyle\sum_{n=0}^{\infty} S_{n+m}^{(2)}(w_0-z_0)M_{n,\ell}^{(2)}(z_0), & i=2,\\ e^{-iv(w_0-z_0)}M_{0,\ell}^{(2)}(z_0), & i=3,\end{cases} \tag{40}$$

$$\widehat{L}_{m,\ell}^{(i)}(w_0)\overset{\text{def}}{=}\begin{cases}\displaystyle\sum_{n=0}^{\infty} S_{n+m}^{(1)}(\overline{w_0-z_0})\widehat{M}_{n,\ell}^{(1)}(z_0), & i=1,\\ \displaystyle\sum_{n=0}^{\infty} S_{n+m}^{(2)}(\overline{z_0-w_0})\widehat{M}_{n,\ell}^{(2)}(z_0), & i=2,\\ e^{iv(\overline{w_0-z_0})}\widehat{M}_{0,\ell}^{(2)}(z_0), & i=3.\end{cases} \tag{41}$$

The series Eq. (39) is referred to as local expansion while formulae Eqs. (40) and (41) are referred to as moment-to-local (M2L) translations. It should be pointed out that Eq. (39) is also valid for expanding integrals that involve G and F kernels.

Finally, from the definitions Eqs. (40) and (41) we obtain a way to transfer M2L expansions from $w_0$ to a new nearby point $w_{0'}$. Replacing $w_0$ by $w_{0'}$ in Eqs. (40) and (41), and assuming that $|w_0-w_{0'}|<r<|z_0-w_0|$, we apply the addition formulae Eqs. (20) and (29) to expand the functions depending on $w_{0'}-z_0$ in terms of functions depending on $w_0-z_0$ and $w_{0'}-w_0$. This process results in

$$L_{m,\ell}^{(i)}(w_{0'})=\begin{cases}\displaystyle\sum_{k=m}^{\infty} R_{k-m}^{(1)}(w_0-w_{0'})L_{k,\ell}^{(1)}(w_0), & i=1,\\ \displaystyle\sum_{k=m}^{\infty} R_{k-m}^{(2)}(w_0-w_{0'})L_{k,\ell}^{(2)}(w_0), & i=2,\\ R_0^{(2)}(w_0-w_{0'})L_{0,\ell}^{(3)}(w_0), & i=3,\end{cases} \tag{42}$$

$$\widehat{L}_{m,\ell}^{(i)}(w_{0'})=\begin{cases}\displaystyle\sum_{k=m}^{\infty} R_{k-m}^{(1)}(\overline{w_0-w_{0'}})\widehat{L}_{k,\ell}^{(1)}(w_0), & i=1,\\ \displaystyle\sum_{k=m}^{\infty} R_{k-m}^{(2)}(\overline{w_{0'}-w_0})\widehat{L}_{k,\ell}^{(2)}(w_0), & i=2,\\ R_0^{(2)}(\overline{w_{0'}-w_0})\widehat{L}_{0,\ell}^{(3)}(w_0), & i=3\end{cases} \tag{43}$$

referred to as local-to-local (L2L) translations.

### 4.3. Error bounds for the multipole expansions

Due to obvious computational constrains, the multipole and local expansions have to be truncated at a finite number of terms when they are applied to approximate BEM integrals. Then, error bounds for the truncated series expansions are essential to control the accuracy of the proposed method, particularly for problems having solutions that exhibit a surface-wave behavior with a frequency depending on the Robin parameter $v$. Therefore, we characterize here how the truncation error depends on the Robin parameter in order to ensure the accuracy of the method for different surface-wave frequencies.

For the sake of simplicity in the analysis we start by introducing the notation

$$\int_{\Gamma_\ell} K(w,z)\varphi(z)d\sigma_z=\frac{\phi^{\ln}(w)}{4\pi}+\frac{\phi^{\mathrm{Ei}}(\overline{w})+\phi^{\mathrm{Ei}}(w)}{2\pi}+\frac{\phi^{\cos}(w)}{2i},$$

where $\phi^{\ln}$ contains the integrals involving logarithmic kernels and their derivatives, $\phi^{\cos}$ does the same for the cosine kernel, and

$$\phi^{\mathrm{Ei}}(\overline{w})=\int_{\Gamma_\ell}\left\{(i\eta v-v_s(z))e^{-iv(\overline{w}-z)}\mathrm{Ei}(iv(\overline{w}-z))-\frac{\eta}{\overline{w}-z}\right\}\varphi(z)d\sigma_z,$$

$$\phi^{\mathrm{Ei}}(w)=-\int_{\Gamma_\ell}\left\{(i\overline{\eta}v+v_s(z))e^{-iv(\overline{z}-w)}\mathrm{Ei}(iv(\overline{z}-w))+\frac{\overline{\eta}}{w-\overline{z}}\right\}\varphi(z)d\sigma_z.$$

Here it should be pointed out that $\phi^{\cos}$ does not actually entail approximations by a series, so it is not considered in the analysis. On the other hand, error bounds for the approximation of $\phi^{\ln}$ can be found in the large amount of literature available on the topic (cf. [17,18,49]), so we focus exclusively on the terms depending on the exponential integral function.

The next proposition states an error bound for the approximation of $\phi^{\mathrm{Ei}}(\overline{w})$ by a truncated multipole expansion.

**Proposition 4.1.** *Let $w, z_0 \in \mathbb{C}_+$ such that $|z-z_0|<r$ and $|w-z_0|>rd$ for all $z\in\Gamma_\ell$ with $r>0$ and $d>1$ (see Fig. 2). Also let $v\in\mathbb{C}$ such that $0\leqslant \arg v\leqslant \pi/2$. Then, the error bound*

$$\begin{aligned}&\left|\phi^{Ei}(\overline{w})-\sum_{n=0}^{p} S_n^{(2)}(\overline{w}-z_0)M_{n,\ell}^{(2)}(z_0)\right|\\ &\quad\leqslant \|\varphi\|_{L^1(\Gamma_\ell)}e^{2|v|r}\left\{\frac{|v|+\|v_s\|_{L^\infty(\Gamma_\ell)}}{p+1}+\frac{1}{r}\right\}\frac{d^{-p}}{d-1}\end{aligned} \tag{44}$$

*holds true for all $p\geqslant 1$, where $S_n^{(2)}$ and $M_{n,\ell}^{(2)}$ are defined in Eqs. (26) and (35), respectively.*

**Remark 4.1.** The error bound Eq. (44) is also valid for the multipole expansion of $\phi^{\mathrm{Ei}}(w)$.

**Proof.** We note first that thanks to the multipole expansion Eq. (34), the error is explicitly given by

$$E=\left|\phi^{\mathrm{Ei}}(\overline{w})-\sum_{n=0}^{p} S_n^{(2)}(\overline{w}-z_0)M_{n,\ell}^{(2)}(z_0)\right|=\left|\sum_{n=p+1}^{\infty} S_n^{(2)}(\overline{w}-z_0)M_{n,\ell}^{(2)}(z_0)\right|. \tag{45}$$

Subsequently, taking into account the assumption $|w-z_0|>rd$ and the definition of $S_n^{(2)}$ given in Eq. (26), we can easily get the bound

$$\begin{aligned}\left|S_n^{(2)}(\overline{w}-z_0)\right|&=\frac{(n-1)!}{|iv(\overline{w}-z_0)|^n}\left|\sum_{k=0}^{n-1}\frac{(iv(z_0-\overline{w}))^k}{k!}\right|\\ &\leqslant\sum_{k=0}^{n-1}\frac{(n-1)!}{k!|v|^{n-k}(rd)^{n-k}},\quad n\geqslant 1.\end{aligned} \tag{46}$$

Likewise, from the definition of $R_n^{(2)}$ given in Eq. (25), and taking into consideration the assumption $|z-z_0|<r$, we achieve a bound for the moments given by

$$\begin{aligned}\left|M_{n,\ell}^{(2)}(z_0)\right|&=\left|\int_{\Gamma_\ell}\left\{\eta R_n^{(2)\prime}(z-z_0)-v_s(z)R_n^{(2)}(z-z_0)\right\}\varphi(z)d\sigma_z\right|\\ &\leqslant\int_{\Gamma_\ell}\left|\left\{(i\eta v-v_s)R_n^{(2)}(z-z_0)+i\eta v R_{n-1}^{(2)}(z-z_0)\right\}\varphi(z)\right|d\sigma_z\\ &\leqslant\|\varphi\|_{L^1(\Gamma_\ell)}\frac{e^{|v|r}|v|^n r^n}{(n-1)!}\left\{\frac{|v|+\|v_s\|_{L^\infty(\Gamma_\ell)}}{n}+\frac{1}{r}\right\},\quad n\geqslant 1.\end{aligned} \tag{47}$$

Therefore, the terms of the series defining the error Eq. (45) can be bounded as

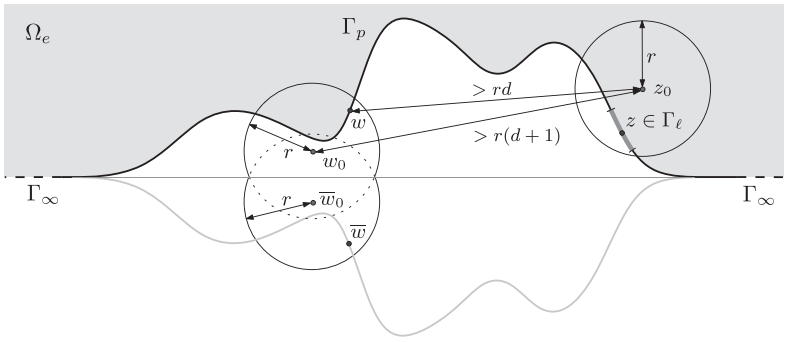


**Fig. 2.** Diagram of the parameters involved in the deduction of the error bounds for the multipole series expansion of the integral $\int_{\Gamma_\ell} \mathrm{K}(w,z)\varphi(z)\mathrm{d}\sigma_z$.

$$\left|\mathrm{S}_n^{(2)}(\overline{w}-z_0)\mathrm{M}_{n,\ell}^{(2)}(z_0)\right| \leqslant \|\varphi\|_{L^1(\Gamma_\ell)}\mathrm{e}^{|v|r}\left\{\frac{|v|+\|v_s\|_{L^\infty(\Gamma_\ell)}}{n}+\frac{1}{r}\right\}\sum_{k=0}^{n-1}\frac{(|v|rd)^k}{k!}d^{-n}.$$

Now, noticing that

$$\sum_{n=p+1}^{\infty}\sum_{k=0}^{n-1}\frac{(|v|rd)^k}{k!}d^{-n} \leqslant \sum_{n=p+1}^{\infty}\sum_{k=0}^{n}\frac{(|v|rd)^k}{k!}d^{-n} = \left(\sum_{n=p+1}^{\infty}d^{-n}\right)\left(\sum_{k=0}^{\infty}\frac{(|v|rd)^k}{k!}d^{-k}\right),$$

we find that

$$E \leqslant \|\varphi\|_{L^1(\Gamma_\ell)}\mathrm{e}^{2|v|r}\left\{\frac{|v|+\|v_s\|_{L^\infty(\Gamma_\ell)}}{p+1}+\frac{1}{r}\right\}\frac{d^{-p}}{d-1},$$

in virtue of the infinite radius of convergence of the exponential series and the fact that $d>1$. □

The next proposition establishes an error bound for local expansion coefficients of $\phi^{\mathrm{Ei}}(\overline{w})$.

**Proposition 4.2.** *Let $w, z_0 \in \mathbb{C}_+$ such that $|z-z_0|<r$ and $|w-z_0|>rd$ for all $z\in\Gamma_\ell$ with $r>0$ and $d>1$ (see Fig. 2). Also let $v\in\mathbb{C}$ such that $0\leqslant \arg v \leqslant \pi/2$. Then, the following error bound*

$$\left|L_{m,\ell}^{(2)}(\overline{w}_0)-\sum_{n=0}^{p}S_{n+m}^{(2)}(\overline{w}_0-z_0)M_{n,\ell}^{(2)}(z_0)\right| \leqslant \frac{\|\varphi\|_{L^1(\Gamma_\ell)}e^{|v|r(1+d)}}{|v|^m r^m}\left\{\frac{|v|+\|v_s\|_{L^\infty(\Gamma_\ell)}}{p+1}+\frac{1}{r}\right\}\frac{(m+p)!}{p!}\frac{(d-1)^{m+1}}{d^{2m+p+2}} \tag{48}$$

*holds true for all $p\geqslant 1$ and $m\geqslant 1$, where $S_n^{(2)}, M_{n,\ell}^{(2)}$, and $L_{n,\ell}^{(2)}$ are defined in Eqs. (26), (35), and (40), respectively. For the case $m=0$ and $p\geqslant 1$ the corresponding error bound is given by Eq. (44).*

**Remark 4.2.** The error bound Eq. (48) is also valid for $\widehat{\mathrm{L}}_{m,\ell}^{(2)}(\overline{w}_0)$.

**Proof.** Due to the definition Eq. (40), we have that the error can be explicitly expressed as

$$E_m = \left|\mathrm{L}_{m,\ell}^{(2)}(\overline{w}_0)-\sum_{n=0}^{p}\mathrm{S}_{n+m}^{(2)}(\overline{w}-z_0)\mathrm{M}_{n,\ell}^{(2)}(z_0)\right| = \left|\sum_{n=p+1}^{\infty}\mathrm{S}_{n+m}^{(2)}(\overline{w}-z_0)\mathrm{M}_{n,\ell}^{(2)}(z_0)\right|. \tag{49}$$

Next, considering the bounds Eqs. (46) and (47), we get that

$$\left|\mathrm{S}_{n+m}^{(2)}(\overline{w}_0-z_0)\mathrm{M}_{n,\ell}^{(2)}(z_0)\right| \leqslant \|\varphi\|_{L^1(\Gamma_\ell)}\mathrm{e}^{|v|r}\left\{\frac{|v|+\|v_s\|_{L^\infty(\Gamma_\ell)}}{n}+\frac{1}{r}\right\} \times \frac{(n+m-1)!}{(|v|r)^m d^{n+m}(n-1)!}\sum_{k=0}^{n+m-1}\frac{(|v|rd)^k}{k!}.$$

Consequently, the error is bounded by the series

$$E_m = \left|\sum_{n=p+1}^{\infty}\mathrm{S}_{n+m}^{(2)}(\overline{w}_0-z_0)\mathrm{M}_{n,\ell}^{(2)}(z_0)\right| \leqslant \frac{\|\varphi\|_{L^1(\Gamma_\ell)}\mathrm{e}^{|v|r(1+d)}}{|v|^m r^m d^m}\left\{\frac{|v|+\|v_s\|_{L^\infty(\Gamma_\ell)}}{p+1}+\frac{1}{r}\right\}\sum_{n=p+1}^{\infty}\frac{(n+m-1)!}{(n-1)!}d^{-n}. \tag{50}$$

Now, let us note that the last term above admits the representation

$$\sum_{n=p+1}^{\infty}\frac{(n+m-1)!}{(n-1)!}\varrho^n = \frac{(m+p)!}{p!}\varrho^{p+1}{}_2F_1(m+p+1,1;p+1;\varrho), \quad 0<\varrho=d^{-1}<1, \tag{51}$$

where ${}_2F_1$ is the Gauss hypergeometric function (cf. [45]). Then, from [52, Theorem 1.10] we get the inequality

$$\frac{m!(m+p+1)!}{(2m+p+1)!} < \frac{{}_2F_1(m+p+1,1;p+1;\varrho)}{(1-\varrho)^{-m-1}} < 1,$$

which is valid for all $m\geqslant 1$. From here we find that the error bound

$$E_m \leqslant \frac{\|\varphi\|_{L^1(\Gamma_\ell)}\mathrm{e}^{|v|r(1+d)}}{|v|^m r^m}\left\{\frac{|v|+\|v_s\|_{L^\infty(\Gamma_\ell)}}{p+1}+\frac{1}{r}\right\}\frac{(m+p)!}{p!}\frac{(d-1)^{m+1}}{d^{2m+p+2}}$$

is valid for all $m\geqslant 1$. Finally, for the case $m=0$ the error bound follows directly from the fact that $\phi^{\mathrm{Ei}}(\overline{w})=\mathrm{L}_{0,\ell}^{(2)}(\overline{w}_0)$ and the proof of Proposition 4.1. □

The next proposition establishes an error bound for the local expansion of $\phi^{\mathrm{Ei}}(\overline{w})$.

**Proposition 4.3.** *Let the points $w, w_0$ and $z_0$ in $\mathbb{C}_+$ be such that $|w-w_0|<r, |z-z_0|<r$ and $|w_0-z_0|>r(d+1)$ for all $z\in\Gamma_\ell$, where $r>0$ and $d>1$ (see Fig. 2). Also let $v\in\mathbb{C}$ such that $0\leqslant\arg v\leqslant\pi/2$. Then, the error bound*

$$\left|\phi^{Ei}(\overline{w})-\sum_{m=0}^{p}R_m^{(2)}(\overline{w_0-w})L_{m,\ell}^{(2)}(\overline{w}_0)\right| \leqslant \|\varphi\|_{L^1(\Gamma_\ell)}e^{|v|r(1+d)}\left\{\frac{1}{rd}+\frac{|v|+\|v_s\|_{L^\infty(\Gamma_\ell)}}{p+1}\right\}\frac{d^{-p}}{d-1} \tag{52}$$

*holds true for all $p \geqslant 1$, where $R_m^{(2)}$ and $L_{m,\ell}^{(2)}$ are defined in Eqs. (25) and (40), respectively.*

**Remark 4.3.** The error bound Eq. (52) is also valid for $\phi^{\mathrm{Ei}}(w)$.

**Proof.** First we observe that thanks to the local expansion Eq. (39), the error can be explicitly expressed as

$$E = \left| \phi^{\mathrm{Ei}}(\overline{w}) - \sum_{m=0}^{p} \mathrm{R}_m^{(2)}(\overline{w_0 - w})\mathrm{L}_{m,\ell}^{(2)}(\overline{w}_0) \right| = \left| \sum_{m=p+1}^{\infty} \mathrm{R}_m^{(2)}(\overline{w_0 - w})\mathrm{L}_{m,\ell}^{(2)}(\overline{w}_0) \right|.$$

In order to find bounds for the terms in the series defining the error, we compare the addition formula for the functions $\mathrm{S}_n^{(2)}$ given in Eq. (29), the definition of the moments Eq. (35), and the M2L formula Eq. (40), to realize that

$$\mathrm{L}_{m,\ell}^{(2)}(\overline{w}_0) = -\int_{\Gamma_\ell} \left\{ \eta \mathrm{S}_m^{(2)\prime}(\overline{w}_0 - z) + v_s(z)\mathrm{S}_m^{(2)}(\overline{w}_0 - z) \right\} \varphi(z)\mathrm{d}\sigma_z.$$

Now, from the definition of $\mathrm{S}_n^{(2)}$ in can be inferred that

$$\mathrm{S}_m^{(2)\prime}(z) = -\mathrm{i}\nu \left\{ \mathrm{S}_m^{(2)}(z) + \mathrm{S}_{m+1}^{(2)}(z) \right\}, \quad m \geqslant 1.$$

Therefore, by means of the bound for $\mathrm{S}_n^{(2)}$ given in Eq. (46), we achieve that

$$\left| \mathrm{S}_m^{(2)\prime}(\overline{w}_0 - z) \right| \leqslant \frac{m!\mathrm{e}^{|\nu| rd}}{|\nu|^m (rd)^m} \left( \frac{|\nu|}{m} + \frac{1}{rd} \right)$$

because due to the triangular inequality we have that $|w_0 - z| > rd$ under the assumptions that $|w_0 - z_0| > r(d+1)$ and $|z - z_0| < r$. Accordingly, we get the bound

$$\left| \mathrm{L}_{m,\ell}^{(2)}(\overline{w}_0) \right| \leqslant \|\varphi\|_{L^1(\Gamma_\ell)} \frac{m!\mathrm{e}^{|\nu| rd}}{|\nu|^m (rd)^m} \left\{ \frac{1}{rd} + \frac{|\nu| + \|v_s\|_{L^\infty(\Gamma_\ell)}}{m} \right\},$$

which, together with

$$\left| \mathrm{R}_m^{(2)}(\overline{w_0 - w}) \right| \leqslant \frac{|\nu|^m r^m \mathrm{e}^{|\nu| r}}{m!}$$

leads to

$$\left| \mathrm{R}_m^{(2)}(\overline{w_0 - w})\mathrm{L}_{m,\ell}^{(2)}(\overline{w}_0) \right| \leqslant \|\varphi\|_{L^1(\Gamma_\ell)} \frac{\mathrm{e}^{|\nu| r(1+d)}}{d^m} \left\{ \frac{1}{rd} + \frac{|\nu| + \|v_s\|_{L^\infty(\Gamma_\ell)}}{m} \right\}.$$

Finally, taking into consideration that $m^{-1} \leqslant (p+1)^{-1}$ when $m \geqslant p+1$, we get the bound

$$E \leqslant \|\varphi\|_{L^1(\Gamma_\ell)} \mathrm{e}^{|\nu| r(1+d)} \left\{ \frac{1}{rd} + \frac{|\nu| + \|v_s\|_{L^\infty(\Gamma_\ell)}}{p+1} \right\} \frac{d^{-p}}{d-1}. \qquad \square$$

### 4.4. FM-BEM algorithm

In this subsection we give the details of the FM-BEM algorithm, which thanks to the previously obtained multipole and local expansions, corresponds, in general terms, to the classic adaptive algorithm for potential problems (cf. [21,38,53]).

For a given problem's domain $\Omega_e$, we discretize the perturbed part of its boundary $\Gamma_p$ in the same way as in the conventional BEM approach, that is, assuming it given by $\Gamma_p = \bigcup_{\ell=1}^{N} \Gamma_\ell$ where each $\Gamma_\ell$ is a straight line segment. Subsequently we construct a square placed on $\overline{\mathbb{R}_+^2}$ containing all the $N$ boundary segments composing $\Gamma_p$, which is the 0 level cell. Then, an adaptive data structure is built recursively by dividing the 0 level cell into four child cells of level 1. If the cell under consideration contains no segments, i.e., no middle point of a segment is contained in the cell, it is immediately forgotten. If the cell contains fewer than $s$ segments—where $s$ is an appropriately chosen positive integer—it is not subdivided further and is considered a leaf cell. Otherwise, it is regarded as a parent cell and is subdivided into four child cells. This procedure is then repeated for each one of the following cells.

Let us now introduce some important definitions. Two cells at the same level $l$ are said to be adjacent cells at level $l$ if they have at least one common vertex. Two cells are said to be well separated at level $l$ if they are not adjacent at level $l$ but their parent cells are adjacent at level $l-1$. The list of all well-separated cells from a level $l$ cell $c$ is called the interaction list of $c$. Cells at the same level of $c$, are called to be far cells of $c$ if their parent cells are not adjacent to the parent cell of $c$. Finally, we generalize the notion of the adjacency for leaf cells at different levels. Accordingly, two leaf cells $c_1$ and $c_2$ at levels $l_1$ and $l_2$ ($l_1 < l_2$) respectively, are adjacent, if the level $l_1$ cell to which $c_2$ belongs is adjacent to $c_1$ at level $l_1$.

The algorithm for the matrix–vector multiplication between $\boldsymbol{K}$ and a complex vector $\boldsymbol{v} \in \mathbb{C}^N$ is then carried out through the following steps:

1. *Upward pass*. Multipole moments are calculated for each cell at all levels $l \geqslant 2$ for $n = 0, \ldots, p$. Starting from the biggest level, the moments are computed first for each leaf cell $c$ applying directly Eqs. (35) and (36), taking $z_0$ equal to the center of $c$; considering $\varphi(z) = \sum_j v_j \varphi_j(z)$ where the sum is taken over all the basis functions $\varphi_j$ having support on $\ell$; and adding the contributions of all the segments $\ell$ contained in $c$. For a parent cell, the moments are computed by shifting the moments of its child cells to the parent cell center $z_0'$ by using M2M translation formulae Eqs. (37) and (38). Adding the contributions of all its child cells we achieve the moments of $c$. We continue the M2M translations upward until the level 2 is reached.
2. *Downward pass*. Local expansion coefficients for $m = 0, \ldots, p$ are computed on all cells starting from level 2 and tracing the tree structure downward. The local coefficients associated with a cell $c$ is the sum of the contributions of cells in its interaction list and cells far from $c$. The contributions of cells in the interaction list are calculated through the M2L translation formulae Eqs. (40) and (41), taking $w_0$ as the center of $c$ and considering the moments of all the cells in the interaction list. The contributions of far cells are calculated by using L2L translations formulae equations (42) and (43), with the local coefficients at the expansion point $w_0'$, the center of the parent cell of $c$, being shifted to $w_0$, the center of $c$. For a cell $c$ at level 2, we use only the M2L translation formulae to compute the coefficients of the local expansion.
3. *Evaluation of the matrix–vector product*. For a colocation point $w_i$ in a leaf cell $c$, we evaluate the associated $i$th coordinate of $\boldsymbol{K}\boldsymbol{v}$ as the sum of two parts. The contributions from segments in the leaf $c$ and its adjacent cells, are evaluated directly in the way of the conventional BEM. The contributions from all other segments are obtained from the local expansion Eq. (39) achieved by taking $w = w_i$ and using the local coefficients of $c$ computed in the downward pass. The remaining coordinates are computed in exactly the same way.

Let us observe that no interactions between well separated cells are computed by using multipole expansions. Therefore, we are allowed to choose $d = 2$ in Propositions 4.1–4.3 (cf. [18,49,53]) and consequently all the expansions upon which the algorithm is based are valid as well as error bounds Eqs. (44), (48), and (52). Furthermore, it can be inferred from here that given a Robin parameter, a discretization of the perturbed boundary, and a quad-tree structure, the truncation error is bounded by $C2^{-p}, C > 0$. Therefore, like the classical FMM algorithm for particle simulations, in order to obtain a relative precision $\epsilon, p$ would have to be chosen of order $|\log_2(\epsilon)|$.

As in the classical adaptive FM-BEM for potential problems in the plane (cf. [53,38]), it can be estimated that the resulting algorithm for a matrix–vector product exhibits an asymptotic computational complexity of $\mathcal{O}(N)$. Accordingly, the solution of the linear system Eq. (12) through an iterative algorithm would present the same computational complexity if a moderate number of iterations ($\ll N$) are required to achieve an approximate solution within a prescribed tolerance.

## 5. Numerical examples

In this section we present some examples to demonstrate the efficiency and accuracy of the FM-BEM for solving potential problems defined in locally perturbed half-planes with a Robin boundary condition. The algorithm was implemented in Fortran 95 and the codes have been tested in a laptop PC with an Intel 2.4 GHz CPU and 2 GB RAM. In all the examples we use constant basis functions and collocation points placed at the middle of each boundary segment. The iterative method for solving the linear algebraic system is the version of the GMRES presented in [53] which is based on the reverse communication mechanism for the matrix–vector product. The exponential integral function is numerically evaluated by using the subroutines of Amos [55] and Morris [56], whereas the functions $S_n^{(2)}$ are computed through the recurrence relation Eq. (22), which has been proved to be stable [50].

### 5.1. Benchmark problem

First of all, to validate the proposed FM-BEM method, we consider as benchmark problem a domain $\Omega_e$ taken as the exterior of a half-circle of radius $R = 1$ centered at the origin. The perturbed boundary $\Gamma_p$ is then given by the upper half-circle, and the Robin parameter $\nu_s$ is chosen constant throughout $\Gamma$. As boundary data we take

$$f(\mathbf{x}) = -\frac{\partial G(\mathbf{x},\mathbf{z})}{\partial n_{\mathbf{x}}} + \nu_s(\mathbf{x}) G(\mathbf{x},\mathbf{z}),$$

with the source point $\mathbf{z} = (0, 0)$. In this case the exact solution of Eq. (1) is given by

$$u(\mathbf{x}) = -G(\mathbf{x},\mathbf{z}).$$

As the exact solution of the problem is known, we can test the accuracy of the proposed method by comparing the exact solution with the approximate solution through a relative error defined as

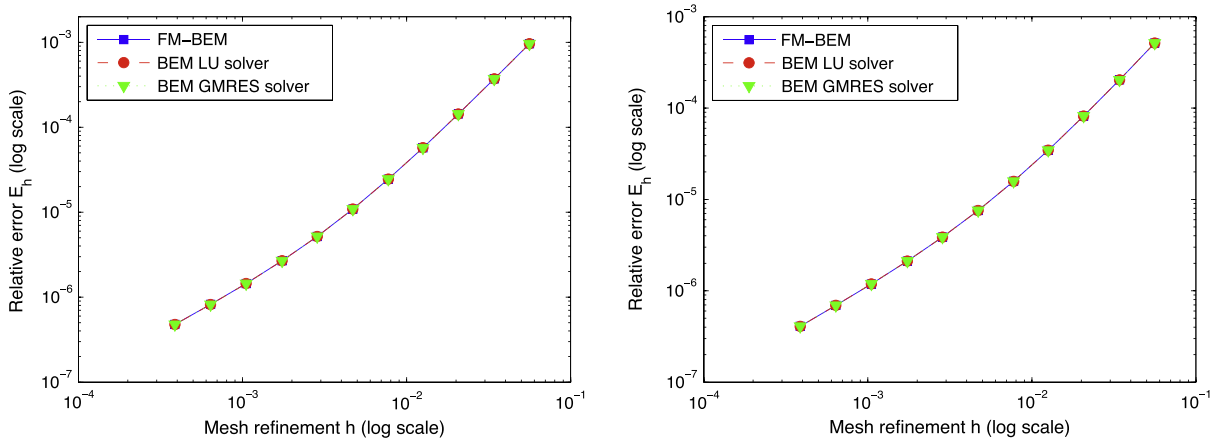


**Fig. 3.** Relative error $E_h$ produced by the FM-BEM and the BEM to solve the benchmark problem.

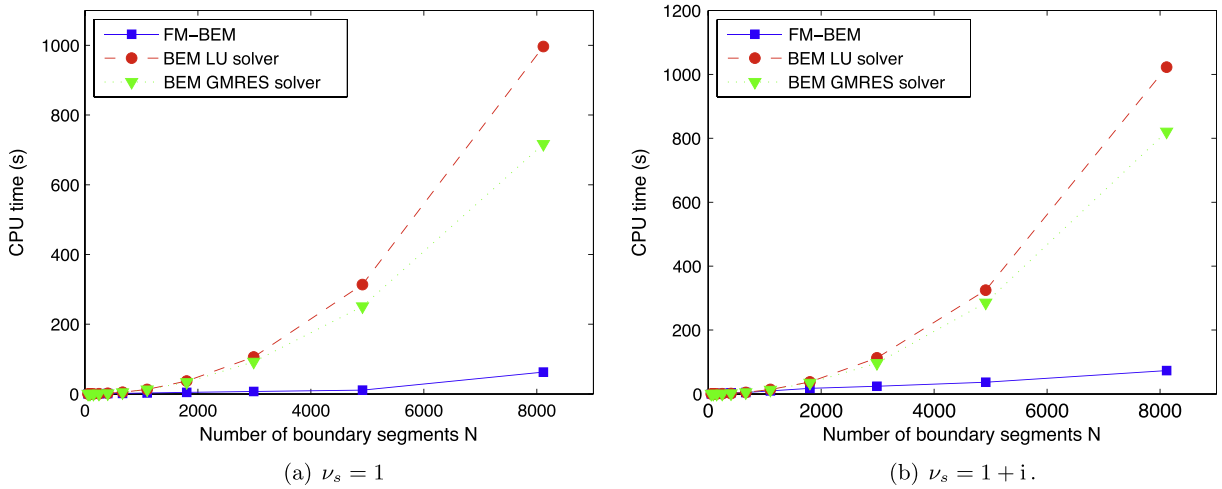


**Fig. 4.** CPU time required by the FM-BEM and the BEM to solve the benchmark problem.

$$E_h = \frac{\|u_h - u\|_{L^2(\Gamma_p)}}{\|u\|_{L^2(\Gamma_p)}}.$$

Figs. 3 and 4 compare the FM-BEM and the conventional BEM using the LU decomposition and the GMRES algorithm for the solution of the linear system stemming from the discretization of the boundary integral equation of the benchmark problem. The results of the FM-BEM were obtained by taking $p = 15$ and $s = 20$. Convergence was reached after 8 GMRES iterations using an error tolerance of 1e-10. Fig. 3(a), (b) compare the error $E_h$ for a real and a complex Robin parameter for different mesh sizes $h$. As can be observed in the results, no accuracy differences can be appreciated between the considered methods. On the other hand, Fig. 4(a), (b) demonstrate the efficiency of the proposed method by comparing the CPU time taken by the FM-BEM and the conventional BEM to solve the benchmark problem for a real and a complex Robin parameter.

### 5.2. A scattering problem

From the linear theory of water-waves (cf. [2]) we know that a one-dimensional plane surface-wave of the form $u_I(\mathbf{x}) = e^{-\nu(ix_1+x_2)}$ is allowed to propagate undisturbed along the flat boundary of an unperturbed half-plane with a Robin parameter $\nu$. Thus, when a compact perturbation of the half-plane is taken into account, the solution of the differential problem Eq. (1) with boundary data

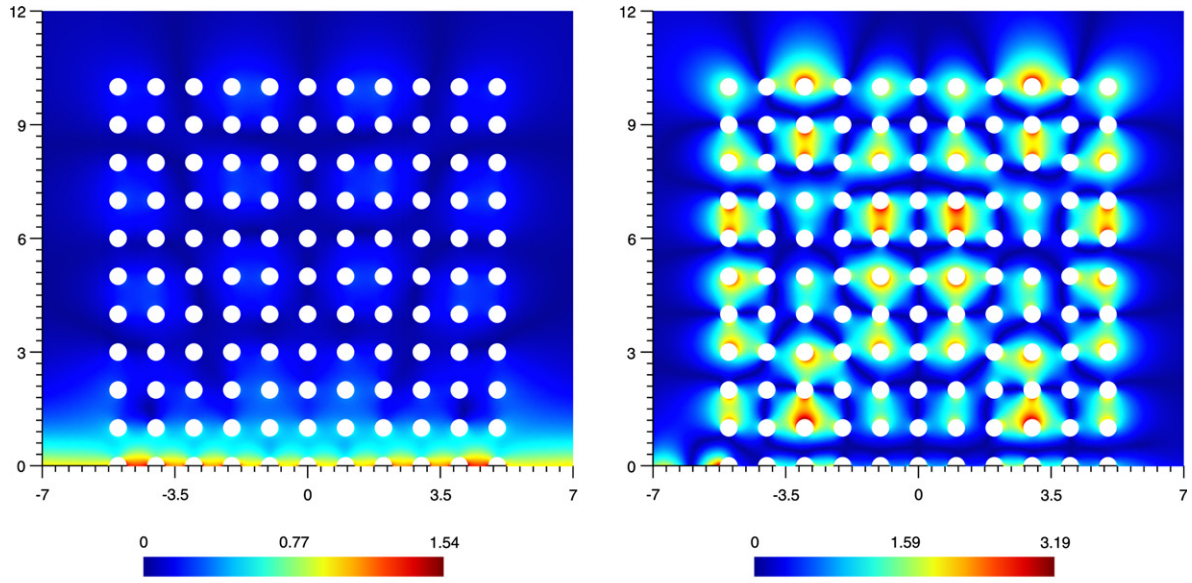


(a) Case $\nu_s = 1$. It was solved in 1231 seconds after 76 GMRES iterations.

(b) Case $\nu_s = 2$. It was solved in 2271 seconds after 150 GMRES iterations.

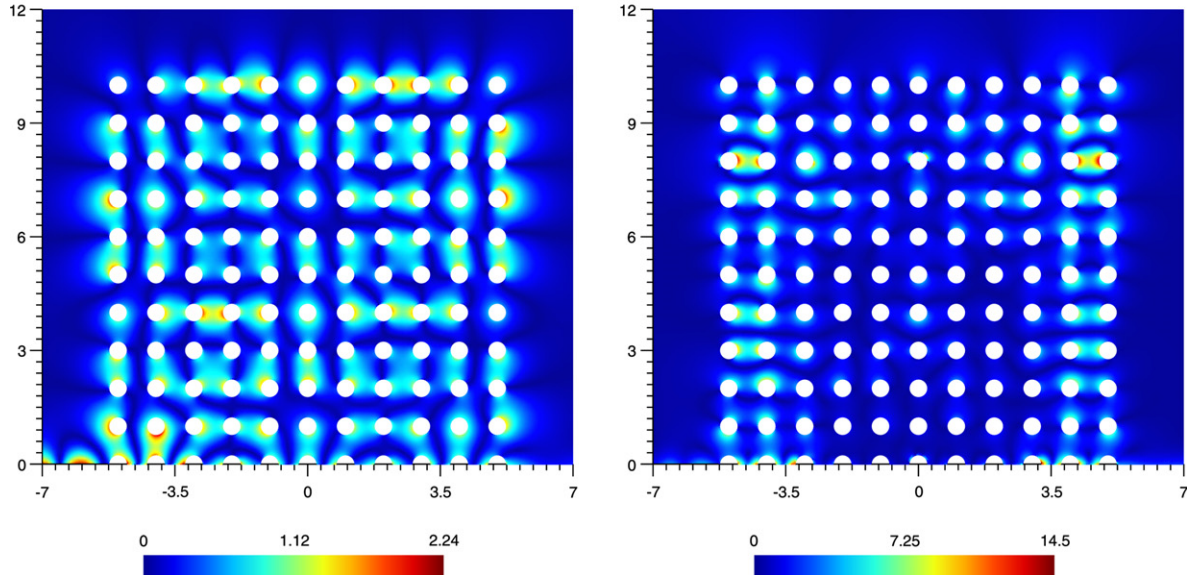


(c) Case $\nu_s = 3$. It was solved in 3197 seconds after 232 GMRES iterations.

(d) Case $\nu_s = 4$. It was solved in 5400 seconds after 410 GMRES iterations.

**Fig. 5.** Plot of $|u_T|$ for four different values of the Robin parameter in a mesh with up to 1e5 nodes.

$$f(\mathbf{x}) = -\frac{\partial u_I(\mathbf{x})}{\partial n} + v_s(\mathbf{x})u_I(\mathbf{x}), \quad \mathbf{x} \in \Gamma$$

represents the scattered field due to obstacles or variations of $v_s$ encountered by the surface incident wave $u_I$.

As an example we consider the scattering by an array of 121 equally spaced cylinders placed in the half-plane, as is shown in Fig. 5. The boundary mesh accounts for up to 100000 nodes. The resulting integral Eq. (9) was solved using the FM-BEM for four different values of the Robin parameter. Fig. 5 depicts the absolute value of the total field $u_T = u_I + u$ for each case. This example clearly demonstrates the efficiency of the FM-BEM for solving large scale problems, despite the large number of GMRES iterations needed to get the desired accuracy in some cases.

It has to be pointed out that the method becomes prohibitively expensive for some values of the Robin parameter $v_s$. Two different factors explain this drawback. On one hand, it is observed that for a fixed number of terms of the multipole expansions the truncation error grows with $v_s$. This phenomenon is captured by the error bounds obtained in Section 4.3 and is related with the appearance high-frequency oscillations of the solution in the neighborhood of the boundary. On the other hand, we notice that the problem may become very ill-conditioned for a countable set of values of the impedance parameter $v_s$ associated with the Steklov eigenvalues of the problem, which seems to be the phenomenon observed in this example. This drawback can be partially suppressed by introducing a suitable preconditioner (cf. [25]) or by modifying the boundary integral equation.

## Acknowledgement

Pedro Ramaciotti was supported by the program MECE Educación Superior (2) PUC0710.

## References

[1] J.V. Wehausen, E.V. Laitone, Surface waves, in: S. Flügge (Ed.), Encyclopedia of Physics, vol. IX, Springer, Berlin, 1960, pp. 446–778.
[2] N. Kuznetsov, V. Maz'ya, B. Vainberg, Linear Water Waves: A Mathematical Approach, first ed., Cambridge University Press, 2002.
[3] C.K. Sollitt, R.H. Cross, Wave transmission through permeable breakwaters, in: Proceedings of the 13th Coastal Engineering Conference, ASCE, 1972, pp. 1827–1846.
[4] K. Sarkar, A. Prosperetti, Effective boundary conditions for the Laplace equation with a rough boundary, in: Proceedings of the Royal Society: Mathematical, Physical and Engineering Sciences, vol. 451, 1942, 1995, pp. 425–452.
[5] M.N. Özisik, Boundary Value Problems of Heat Conduction, International Textbook Co., 1968.
[6] F. Lemczyk, M.M. Yovanovich, Thermal constriction resistance with convective boundary conditions. 1. Half-space contacts, Int. J. Heat Mass Trans. 31 (9) (1988) 1861–1872.
[7] P.M. Morse, K.U. Ingard, Linear Acoustic Theory, in: S. Flügge (Ed.), Encyclopedia of Physics, vol. XI/1, Springer, Berlin, 1961, pp. 1–128.
[8] A. Sommerfeld, Partial Differential Equations in Physics, Academic Press, New York, 1949.
[9] N.G. Green, A. Ramos, A. González, H. Morgan, A. Castellanos, Fluid flow induced by nonuniform ac electric fields in electrolytes on microelectrodes. iii. Observation of streamlines and numerical simulation, Phys. Rev. E 66 (2) (2002) 026305.
[10] C.C. Mei, Numerical methods in water-wave diffraction and radiation, Ann. Rev. Fluid Mech. 10 (1978) 393–416.
[11] R.W. Yeung, Numerical methods in free-surface flows, Ann. Rev. Fluid Mech. 14 (1982) 395–442.
[12] F. John, On the motion of floating bodies I, Commun. Pure Appl. Math. 2 (1949) 13–57.
[13] F. John, On the motion of floating bodies II, Commun. Pure Appl. Math. 3 (1950) 45–101.
[14] P.A. Martin, On the null-field equations for water-wave radiation problems, J. Fluid Mech. 113 (1981) 315–332.
[15] R. Hein, M. Durán, J.-C. Nédélec, Explicit representation for the infinite-depth two-dimensional free-surface Green's function, SIAM J. Appl. Math. 70 (7) (2010) 2353–2372.
[16] N. Nishimura, Fast multipole accelerated boundary integral equation methods, ASME Appl. Mech. Rev. 55 (4) (2002) 299–324.
[17] V. Rokhlin, Rapid solution of integral equations of classical potential theory, J. Comput. Phys. 60 (2) (1985) 187–207.
[18] L. Greengard, V. Rokhlin, A fast algorithm for particle simulations, J. Comput. Phys. 73 (1987) 325–348.
[19] L. Greengard, V. Rokhlin, A new version of the fast multipole method for the Laplace equation in three dimensions, Acta Numer. 6 (1997) 229–269.
[20] L. Shen, Y.J. Liu, An adaptive fast multipole boundary element method for three-dimensional potential problems, Comput. Mech. 39 (2007) 681–691.
[21] Y.J. Liu, N. Nishimura, The fast multipole boundary element method for potential problems: a tutorial, Engrg. Anal. Bound. Elem. 30 (2006) 371–381.
[22] S. Amini, A.T.J. Profit, Multi-level fast multipole solution of the scattering problem, Engrg. Anal. Bound. Elem. 27 (2003) 547–564.
[23] L. Shen, Y.J. Liu, An adaptive fast multipole boundary element method for three-dimensional acoustic wave problems based on the Burton–Miller formulation, Comput. Mech. 40 (2007) 461–472.
[24] M. Bapat, L. Shen, Y.J. Liu, Adaptive fast multipole boundary element method for three-dimensional half-space acoustic wave problems, Engrg. Anal. Bound. Elem. 33 (2009) 1113–1123.
[25] S. Li, Q. Huang, A new fast multipole boundary element method for two dimensional acoustic problems, Comput. Methods Appl. Mech. Engrg. 200 (2011) 1333–1340.
[26] S. Li, Q. Huang, A fast multipole boundary element method based on the improved Burton–Miller formulation for three-dimensional acoustic problems, Engrg. Anal. Bound. Elem. 35 (5) (2011) 719–728.
[27] G. Of, O. Steinbach, W.L. Wendland, Applications of a fast multipole Galerkin in boundary element method in linear elastostatics, Comput. Visual. Sci. 8 (2005) 201–209.
[28] Y.J. Liu, L. Shen, A dual BIE approach for large-scale modelling of 3-D electrostatic problems with the fast multipole boundary element method, Int. J. Numer. Methods Engrg. 71 (2007) 837–855.
[29] Y.J. Liu, A fast multipole boundary element method for 2D multi-domain elastostatic problems based on a dual BIE formulation, Comput. Mech. 42 (2008) 761–773.
[30] L. Greengard, M.C. Kropinski, A. Mayo, Integral equation methods for stokes flow and isotropic elasticity in the plane, J. Comput. Phys. 125 (2) (1996) 403–414.
[31] A.A. Mammoli, M. Ingber, Stokes flow around cylinders in a bounded two-dimensional domain using multipole-accelerated boundary element methods, Int. J. Numer. Methods Engrg. 44 (1999) 897–917.
[32] Y.J. Liu, A new fast multipole boundary element method for solving 2-D Stokes flow problems based on a dual BIE formulation, Engrg. Anal. Bound. Elem. 32 (2008) 139–151.
[33] Y.H. Chen, W.C. Chew, S. Zeroug, Fast multipole method as an efficient solver for 2D elastic wave surface integral equations, Comput. Mech. 20 (1997) 495–506.
[34] M.S. Tong, W.C. Chew, Multilevel fast multipole algorithm for elastic wave scattering by large three-dimensional objects, J. Comput. Phys. 228 (2009) 921–932.
[35] J. Song, C.C. Lu, W.C. Chew, Multilevel fast multipole algorithm for electromagnetic scattering by large complex objects, IEEE Antenn. Propag. Mag. 45 (10) (1997) 1488–1493.
[36] E. Darve, The fast multipole method: numerical implementation, J. Comput. Phys. 160 (1) (2000) 195–240.
[37] N. Geng, A. Sullivan, L. Carin, Multilevel fast-multipole algorithm for scattering from conducting targets above or embedded in a lossy half space, IEEE Trans. Geosci. Remote Sensing 38 (4) (2000) 1561–1573.
[38] Y. Liu, Fast Multipole Boundary Element Method: Theory and Applications in Engineering, first ed., Cambridge University Press, 2009.
[39] F. Ursell, On the heaving motion of a circular cylinder on the surface of a fluid, Quart. J. Mech. Appl. Math. 2 (2) (1949) 218–231.
[40] F. Ursell, On the rolling motion of cylinders in the surface of a fluid, Quart. J. Mech. Appl. Math. 2 (3) (1949) 335–353.
[41] R.C. Thorne, Multipole expansions in the theory of surface waves, Math. Proc. Cambridge Philos. Soc. 49 (1953) 707–716.
[42] F. Ursell, Irregular frequencies and the motion of floating bodies, J. Fluid Mech. 105 (1981) 143–156.
[43] P.A. Martin, Multiple Scattering: Interaction of Time-harmonic Waves with $N$ Obstacles, Cambridge University Press, 2006.
[44] Y. Saad, M.H. Schultz, GMRES: a generalized minimal residual algorithm for solving nonsymmetric linear systems, SIAM J. Sci. Statist. Comput. 7 (3) (1986) 856–869.
[45] M. Abramovitz, I.A. Stegun, Handbook of Mathematical Functions with Formulas, Graphs and Mathematical Tables, Oxford University Press, 1972.
[46] R. Hein, Green's functions and integral equations for the Laplace and Helmholtz operators in impedance half-spaces, Ph.D. thesis, Ecole Polytechnique-Pontificia Universidad Católica de Chile, 2010.
[47] M. McIver, An example of non-uniqueness in the two-dimensional linear water wave problem, J. Fluid Mech. 315 (1996) 257–266.
[49] L.F. Greengard, The Rapid Evaluation of Potential Fields in Particle Systems, The MIT Press, 1988.
[50] W. Gautschi, Computation of successive derivatives of $f(z)/z$, Mathematics of Computation 20 (94) (1966) 209–214.
[51] J.B. Conway, Functions of one Complex Variable, second ed., Springer, 1978.
[52] S. Ponnusamy, M. Vuorinen, Asymptotic expansions and inequalities for hypergeometric functions, Mathematika 44 (2) (1997) 278–301.

[53] J. Carrier, L. Greengard, V. Rokhlin, A fast adaptive multipole algorithm for particle simulations, SIAM J. Sci. Statist. Comput. 9 (4) (1988) 669–686.
[53] V. Frayssé, L. Giraud, S. Gratton, J. Langou, A set of GMRES routines for real and complex arithmetics on high performance computers, Technical report TR/PA/2003/3, CERFACS, 2003.
[55] D.E. Amos, Algorithm 683: a portable FORTRAN subroutine for exponential integrals of a complex argument, ACM Trans. Math. Softw. 16 (1990) 178–182.
[56] P.M. Morris, NSWC Library of mathematics subroutines, Classics in applied mathematics NSWC TR 92-425, Naval Surface Warfare Center Dahlgren Devision, Dahlgren, 1993.